Characterization of acoustic emission signals under 3-point bending test

Characterization of acoustic emission signals under 3-point bending test

B G N Nguyen[1,*], H G Lemu[1,*], O Gabrielsen[2] and I El-Thalji[1]

[1] University of Stavanger, Faculty of Science and Technology, Norway
[2] DNV AS, Offshore Structures, Stavanger, Norway

[*] Corresponding author: ngb.nguyen@stud.uis.no and Hirpa.g.lemu@uis.no

Abstract. This paper summarizes a master's thesis project which explored whether the characteristics of Acoustic Emission Testing (AET) signals can be used to detect yielding in steel samples undergoing a three-point bending test. A subset of existing data from a three-point bending test was exported and used as input. Data was processed by utilizing and developing tools to visualize and analyse the signal characteristics, primarily through a parameter-based approach. Signals were visualized, and parameters were optimized to identify and classify signal types. According to the obtained results, some limitations on classification were experienced due to the length of the hit data recorded. Though the work reported in this article lead to a reliable method for detecting yielding, the developed algorithms were not successful in identifying characteristics that could be used to detect yielding.

1. Introduction

In the North Sea and other parts of the world, an increasing number of offshore jacket platforms have exceeded their original design life. It is important to maintain the structural integrity of jacket platforms as their economic life is extended. On the Norwegian continental shelf (NCS), the platforms at Ekofisk field, for instance, were originally designed to serve for 20 years [1], but in some cases used for twice as long. The field is a good example of the fact that the service life of oil and gas facilities are often significantly longer than what was originally intended. Therefore, there is a need to find and improve methods that can provide safe operation beyond the original service life of the facility.

New inspection techniques have been constantly developed to secure the use of these assets. In the oil and gas industries, some of the important methods can be taken into consideration, such as online monitoring of environmental data, improving analysis tools, developing inspection technologies, re-analysis tools and planning inspection strategy. Current developments of sensor technology to monitor real-time structural conditions opens new opportunities for offshore structures. Improved sensor properties like robustness, accuracy, efficiency and reducing cost shall enhance the capability to capture the structural response with high data quality. For example, offshore jacket structures, that used to support oil and gas exploration and production facilities, need to sufficiently resist the external loads such as gravity loads, environmental loads, accident loads as well as seismic and ice loads at certain sea locations.

Monitoring of Offshore Jacket Structures is typically performed with periodic manual inspections by various Non-Destructive Testing (NDT) techniques based on risk-based inspection (RBI) and mainly done by either Remote Operated Vehicle (ROV) or divers [2]. Inspection is used to characterize the condition of the structure to assess structural failures and take appropriate actions [3]. In the period

between non-destructive inspections, cracks can initiate, propagate, and catastrophic failure can occur due to the conventional testing based on only gathering information periodically. It depends on the inspection frequency, while the acoustic emission (AE) method can potentially detect active cracks if the structure is installed with a continuous monitoring system. In critical welds, remote monitoring is utilized, because conventional NDT techniques cannot provide an early warning of fracture propagation. Continuous monitoring of AE signals is considered to be a monitoring method which can extend the safe use of offshore platforms [4]. It can also – for redundant structures – replace or reduce the extent of traditional inspection activities.

Remote structural integrity monitoring using AET is a method to detect active fatigue cracks and fatigue damage initiation [5]. For instance, condition-based Maintenance (CBM) can utilize sensors to measure assets' status over time in its operation. However, there are some limitations using this method, for instance, it is costly to install the monitoring equipment and operators must be trained properly in order to use the technology effectively and interpret the signals from the sensors. In addition, the sensors might not work in harsher operating environments and can have trouble in detecting fatigue damage [6].

AE signals are detected by deformation/crack growth, which is recorded by sensors placed around an element. In [4], it is reported that the signal amplitude from crack growth can be measured within a distance of up to 5 meters between sensors. According to [4], acoustic emissions are the elastic energy waves released by a material undergoing deformation. When external stress is imposed on a component, AE signals reflect the internal stress redistribution within a material. Here, the stress can be hydrostatic, pneumatic, thermal, or bending. The signal is effective to identify crack growth and propagation during fatigue tests. Signal discrimination between legitimate sources (for instance, cracks, corrosion, weld discontinuities) and spurious noise sources (such as mechanical friction, weather, engines/machinery, loose parts and other marine environments), as well as noise reduction, are significant for a successful application of AE. Signal discrimination and noise reduction are more crucial in applications to detect corrosion activity because in comparison to crack propagation, the corrosion process is slower, and signal strength is weaker [3]. According to Lee et- al. [3] different defects would leave unique characteristic signatures of AE waveform as illustrated in Figure 1. A suitable testing process and analysis procedure for AE data is essential to acquire a dependable level of structural flaw detection for a successful AET application.

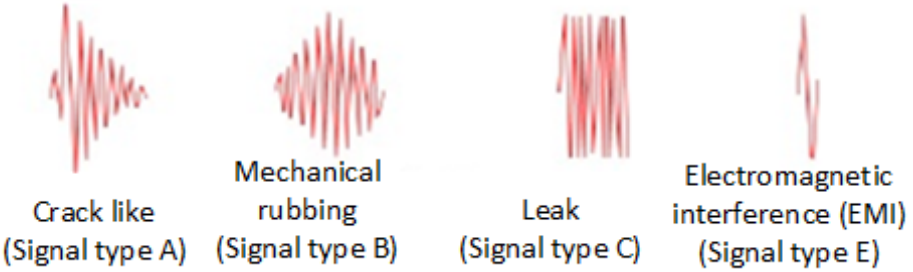

Figure 1. Wave forms (signatures) and their unique representation of type of defect [3].

The goal of the project reported in this article is to study whether the characteristics of signals collected by AET can be used to detect yielding. The work is limited to detection of yielding effect in the specimens based on data from a previous experimental test [7], for which an algorithm was developed in Python to evaluate the signals. Then, the AET data was processed to analyze parameters and signals characteristics.

The article consists of the following sections: Section 2 describes the testing setup and experiments. In Section 3 discussion of the test results on relationship between stress, amplitude and signal strength vs. time, comparison of signal from two sensors and observations of wave types, Fast Fourier Transformation (FFT) of selected signals and wave statistics across several tests are presented. Finally, some conclusions are drawn up based on the results.

2. Experiment

2.1. Materials and experimental set-up

The experimental part of the work reported in this article is based on the selected data collected in a previous master's thesis [7]. In this experiment, a flat steel quality S355J2, according to EN 10025-2 [8] and NORSOK M120 MDS-Y05 [9], was used. The sample dimensions are given in Table 1

Table 1. Dimensions of specimens used in the experiment [10].

Specimen samples	Thickness (mm)	Width (mm)	Length (mm)
A1 (with coating)	14,74	30,10	500
A3N (without coating)	14,72	29,82	500
B1N (without coating)	19,76	29,61	500
B2NR (Reversed, without coating)	29,40	19,74	500

The test specimens A1, B1N and A3N were tested under a normal force that was applied on the width surface. In the case of A3N specimen, a fan was attached as an external noise source that has specific frequency (44 – 54 dB and 55 – 138 kHz). The specimen B2NR, i.e., reversed dimension of sample B2N, was tested under a normal force on the width surface (29,4 mm) with thickness 19,74 mm. The experiment, in this case, was repeated on the same B2N specimen with the force that was applied in different side of the specimen. The reason to do this was because the specimen would be deformed after the first test. Then, in the second attempt, the specimen would be plastified and therefore, different AE results would be recorded and analyzed [7].

A 3-point bending test (Figure 2(a)) was conducted at the desired load using a test machine (Figure 2 (b) [7]) that allows a complex combination of forces including tension, compression and shear when it bends or flexes. The data used in this work was collected from AEwin software (given access by DNV) by exporting from the experiments that were done in [7]. For each of the experiments, there were multiple files that cover relative timestamps and signal amplitude. Due to AEwin software setup, each hit contains 1024 data points. The signal and time units in .csv file were recorded in volts (V) and seconds (s), which were subsequently converted into micro volts (μV) and microseconds (μs) to easily interpret the signal as the interval between the data points in the .csv files are 0.1 μs (logging frequency).

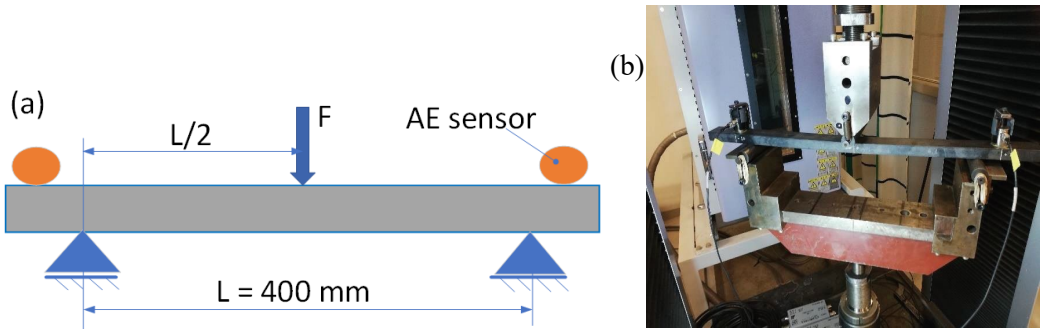

Figure 2. (a) Illustration of bending test on steel specimen (b) Set-up of 3-point bending machine.

2.2. Parameter-based signal analysis

Among the two approaches to signal analysis, i.e., parameter-based and signal-based, the aforementioned approach was used in this study because signal-based approach demands advanced backgrounds. The data analysis of the experimentally recoded signal was programmed in Python, which allows visualization of the results. The developed Python code consists of three programs (1) Process Signal – to collect and connect the data from AEwin (2) Signal Output – to help in illustrating the complete waveform of each experiment without repeating signal processing, and (3) Display Detected

Waveform – to process detected waveforms and export plots of the waveforms. The block diagram in Figure 3 shows the workflow of the signal processing scheme.

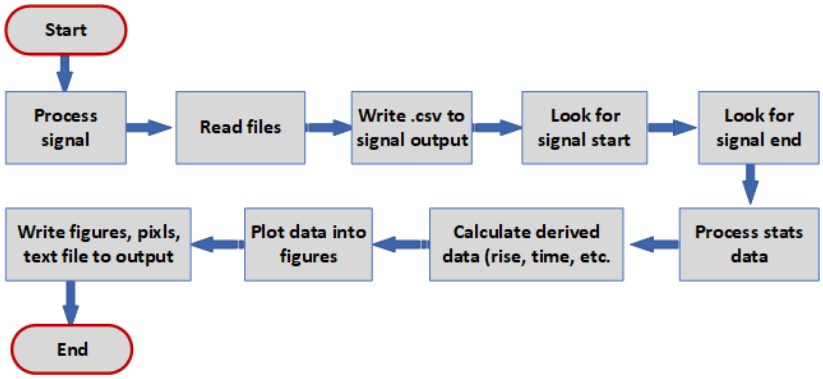

Figure 3. Block diagram (flowchart) of signal processing.

3. Results and discussion

As mentioned earlier, the investigation was conducted by parameter-based characterization of the signal waveform, such as rise duration, signal duration, peak duration, fall duration etc. (illustrated in Figure 4). It involved changing the parameters (threshold, peak threshold and zero duration), executing the program and reviewing the results multiple times until the output showed an identifiable classification of signal types. For example, if the threshold value was set too low, the waveform would be selected from start to end duration, while nothing would be selected if set too high. Zero duration also has a significant impact on selecting the signal; this value determines how long the signal can drop below the threshold before the signal is ended. If too low, crucial signals could be terminated early and if set too high, signals could get merged and not properly classified.

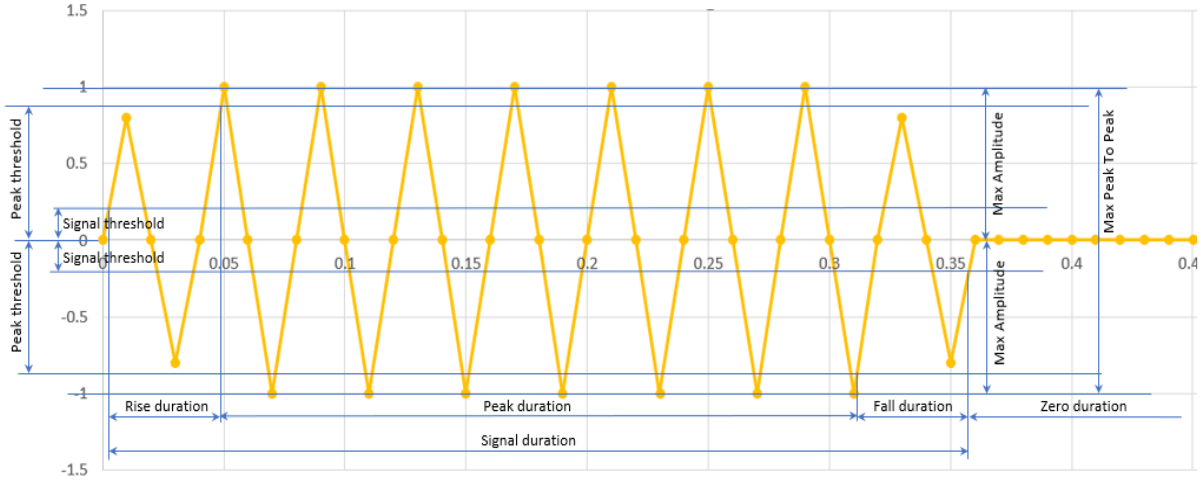

Figure 4. Illustration of waveform characteristics (parameters such as: duration, rise duration, fall duration, peak duration, signal threshold, peak threshold, max amplitude).

During this process, it was discovered that a fixed threshold value would not work efficiently across the merged data as the signal amplitude varied considerably. To combat this problem, the threshold and peak threshold values were changed to be a percentage of the absolute maximum signal amplitude in the set of data points, for example 10% of 1000 µV. Then, the threshold value for this set would become 100 µV. This change gave better results overall, but also resulted in selecting some weak signals that were not of interest.

After experimenting with different values for these three parameters, most of the tests were done by setting threshold value to 10%, peak threshold to 80% and zero duration to 12 µs, though it was understood that zero duration is too short, and it is not physical time. During analysis, specimen B1 was

the main sample used for evaluating signal data. In this section, the relationship between stress, signal strength and amplitude vs. time were studied, and the waveform output from the developed program was discussed. Derived parameters (include duration, rise duration, fall duration, peak duration, max amplitude, frequency) from the output of signal waveforms were evaluated to have a better understanding of the signal characteristics.

3.1. Relationship of stress, amplitude and signal strength with time

Figures 5 (a), (b) and (c) depict the variation of stress, amplitude and signal strength as a function of time for the tested specimens A1, A3N, B1 and B2NR, respectively. As shown in all cases, the signal activity increases, both in number and signal strength, the closer one gets to the yield value. This high activity or intensity, which can be measured as energy, signal strength, absolute energy or similar per time unit, can be used to determine whether yielding occurs or not. From the plots, the number of signals started to increase after 240 s in A1, 220 s in B1 and 100 s in B2NR. This is because specimen A1 had a preservation coating layer, and the cracking of this generated significantly more signal data during the test. B2 is a reversed specimen, and it took lesser time to get to the yield point, and the signal strength was also weaker than the other specimens since it was already deformed once before this test was done.

Since this approach is not very precise, an effort was made to look further into the details of the signal waveform to check for indicators of material deformation. The signal strength itself is not a good indicator as the sensor proximity can affect this condition. Number of signals per time unit is not precise either as can be seen from the high number of signals observed in A1 which was due to the coating layer cracking and not only yielding [7]. Identifying many waveforms of a specific type around the same time can be a solution for this obstacle.

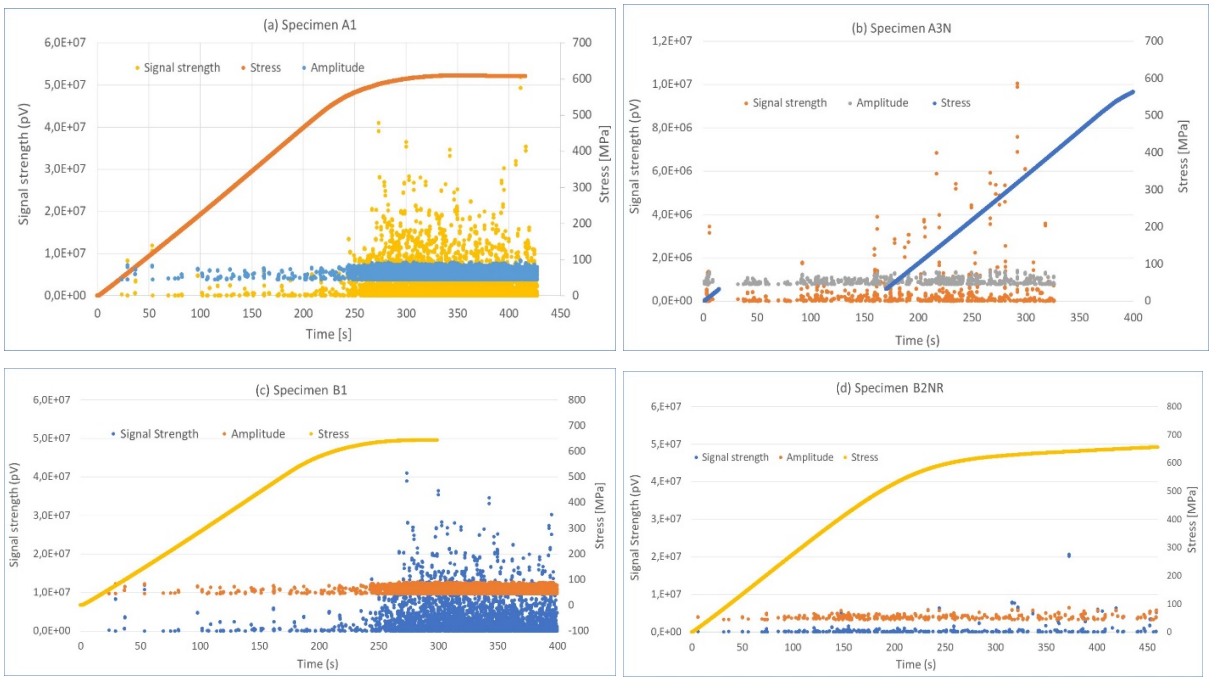

Figure 5. Plots of stress, amplitude and signal strength vs time for (a) Specimen A1, (b) Specimen B1 and (c) Specimen B2NR.

3.2. Comparison of signal from two sensors

Results from the scatter plot and waveform plot, in Figure 6 and Figure 7, respectively, show that signal type A, which has a crack like wave-form (Figure 1B), is the most identified signal during the three-point bending test. Specimen A1 generated a multitude of signal type B, C and E, while specimen B1 showed much less activity. This discrepancy is most likely caused by A1 having a coating layer that

rubs or cracks open during material deformation as the specimens are the same material and dimensions [16]. The majority of signals are of type A in both test A1 and B1, and the algorithm is not able to identify the difference between cracking in coating and the material yielded/deformed.

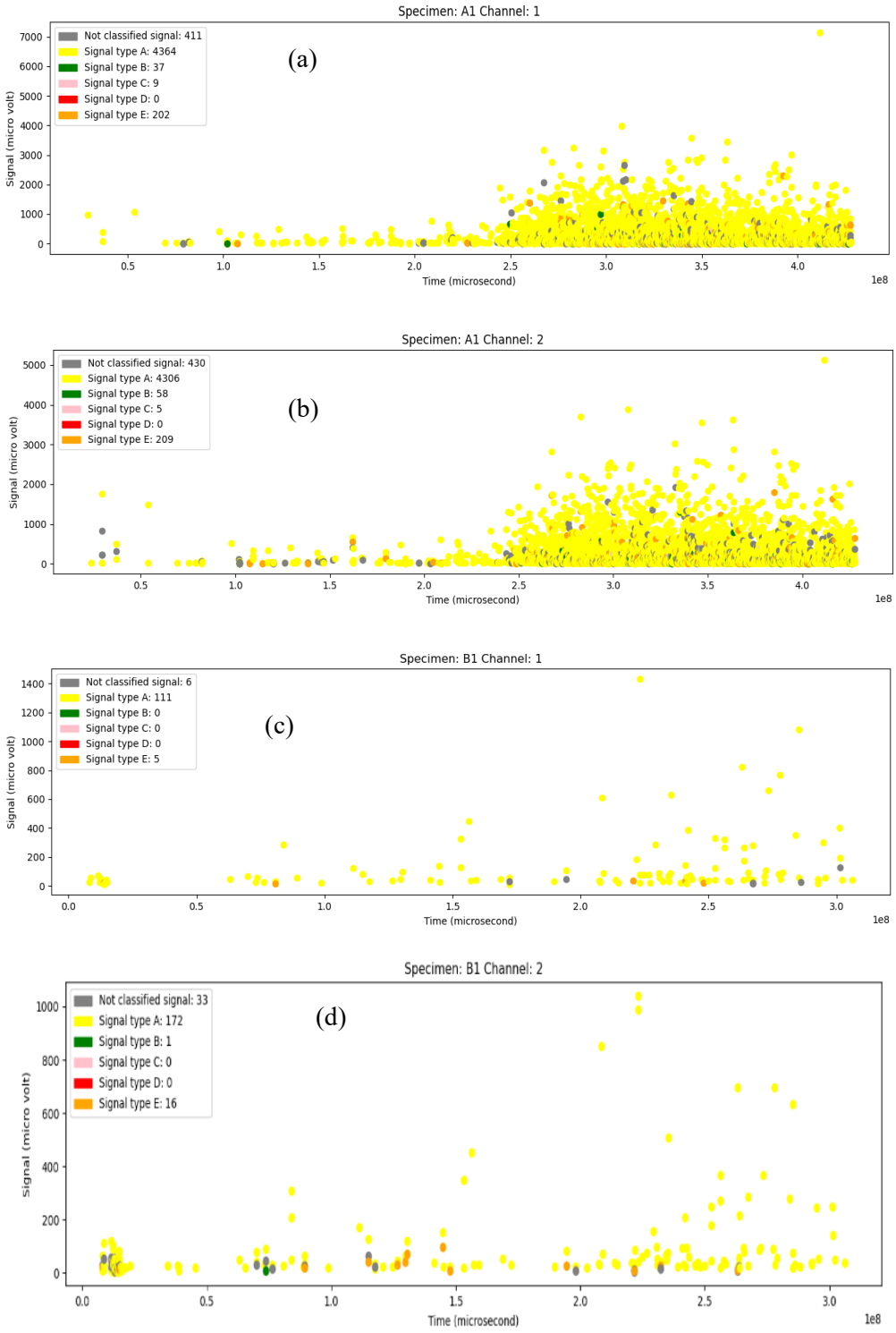

Figure 6. Scatter plot from (a) Test A1, Channel 1 (b) Test A1, Channel 2, (c) Test B1, Channel 1 and (d) Test B1, channel 2.

Comparing the waveform plot in Figure 7 with the relationship between stress, amplitude and signal strength vs time plots discussed earlier (Figure 5), the results show that in test A1, the intensity of activity increases from 240 s and the activity with the highest amplitude is at 411 s. The intensity in test B1 increases from 220 s; the highest amplitude was recorded at 223 s. As stated earlier, the high activity or intensity can be used to determine whether yielding occurs or not.

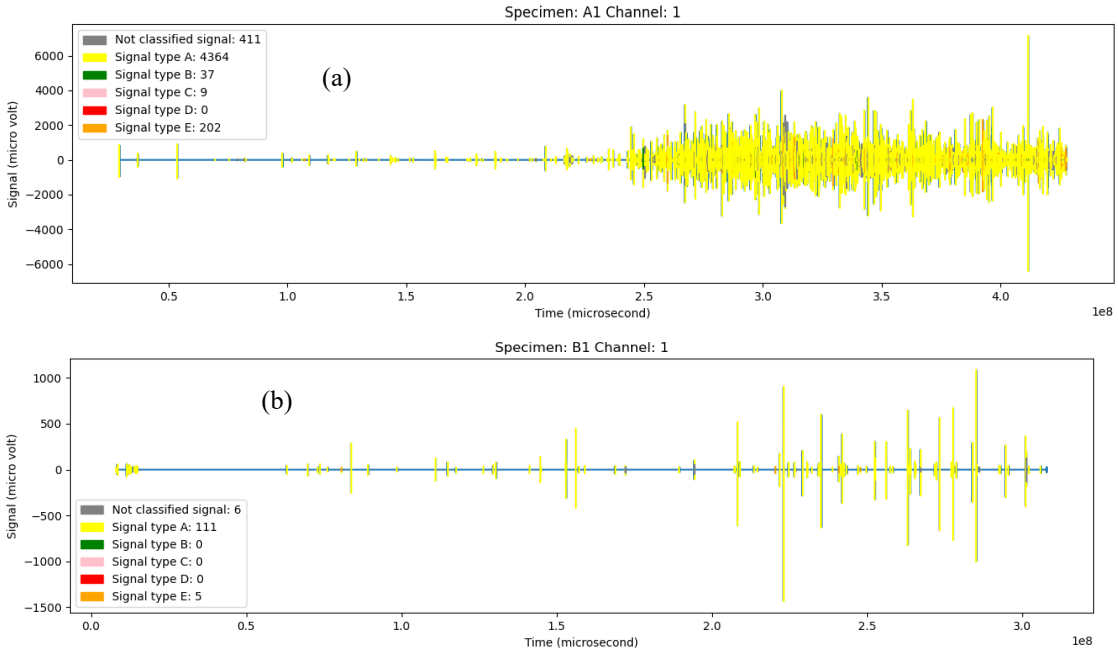

Figure 7. Waveform plot from (a) A1 test and (b) B1 test.

3.3. Observation of waveform types in test B1

Reference of signal types A, B, C and E below (Figure 8) were registered from test B1, with zero duration of 5 μs. It is observed that no shape of signal type D was identified/visualized, which could be due to discontinuity in the signal waveforms that were recorded. This type of signal represents the waveform characteristics of yielding in the material. The expected signal characteristic of type D would be a combination of two A signals where the latter has at least twice the maximum amplitude of the previous.

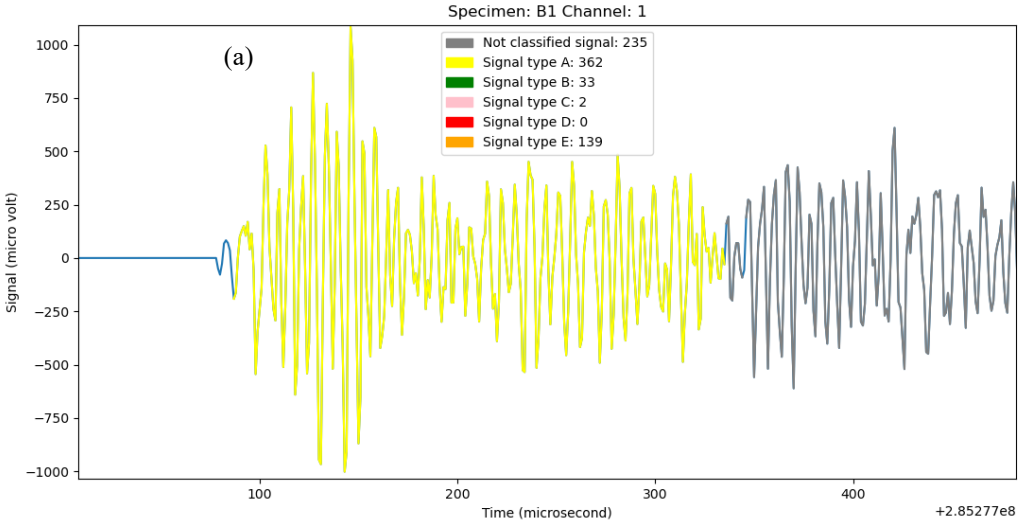

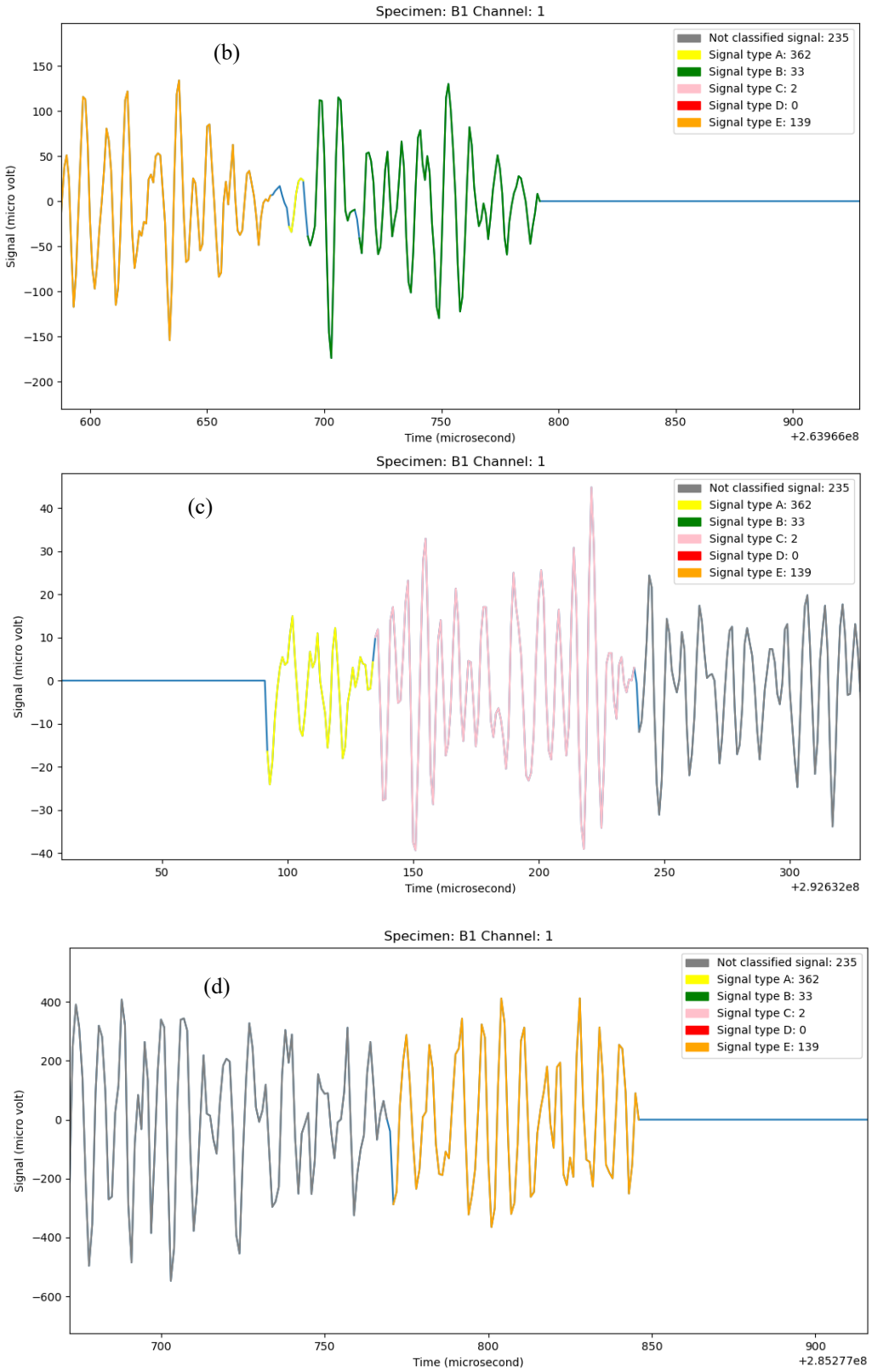

Figure 8. Comparison of the signal types from test B1 (a) Signal type A (in yellow), (b) Signal type B (in green), (c) Signal type C (in pink) and (d) Signal type E (in orange).

As can be observed from plots in Figure 9, signal A rises to a peak value within the first $\frac{1}{3}$ of the duration with a short peak duration. Signal type B contains a diamond shape highlighted in green, with a rise duration equal to fall duration and short peak duration. In contrast, signal type C has a hexagon shape with fast rise and fast fall duration and long peak duration. Signal type E (Figure 9(d)) shows the signal rising to peak value through the last $\frac{2}{3}$ of signal duration. In other words, this signal has long rise duration and short fall duration.

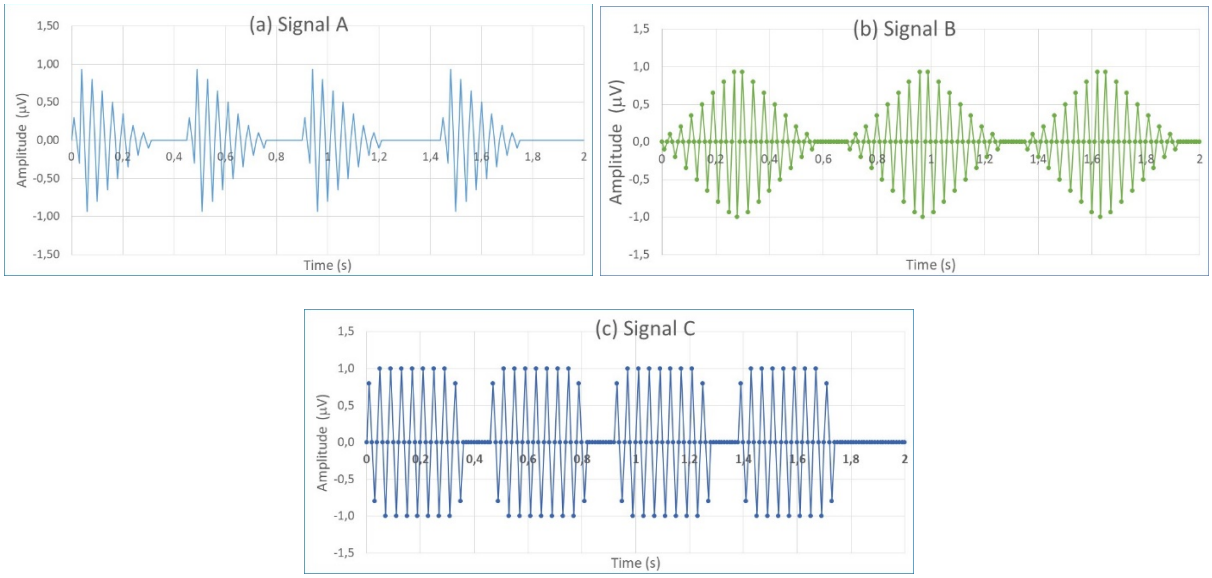

Figure 9: Signal types and wave form characteristics (a) Very fast rise duration, very short peak and long fall duration, (b) Equal rise and fall duration, very short peak duration and (c) Fast rise and fall duration, long peak duration.

3.4. Fast Fourier Transformation of selected signals

The developed signal processing program helps to capture and display detected waveforms with an amplitude greater than a specific threshold and enable the function to examine the frequency content of the signal. Fast Fourier Transformation (FFT) converts the signal in a time-domain to a frequency domain. The transformation breaks down the time-based waveform into sinusoidal terms, with unique intensity, frequency, and phase. FFT can locate intensity of a frequency which can help to determine if the intensity is high around the natural frequency of the material.

For A1 specimen threshold was set at 2000 mV and B1 threshold was set at 500 mV, resulting in numerous waveform plots for each execution. The two figures (Figure 10 and 11) were selected based on the highest absolute signal values for specimens A1 and B1. Results from the signal measured in A1 specimen shows that the intensity spikes around 2 kHz and 15 kHz. In specimen B1, the intensity of the recorded signal increases around 8 kHz and 42 kHz. There is an abundance of interesting data to be analyzed in the frequency domain and time did not allow for in-depth studies in this project.

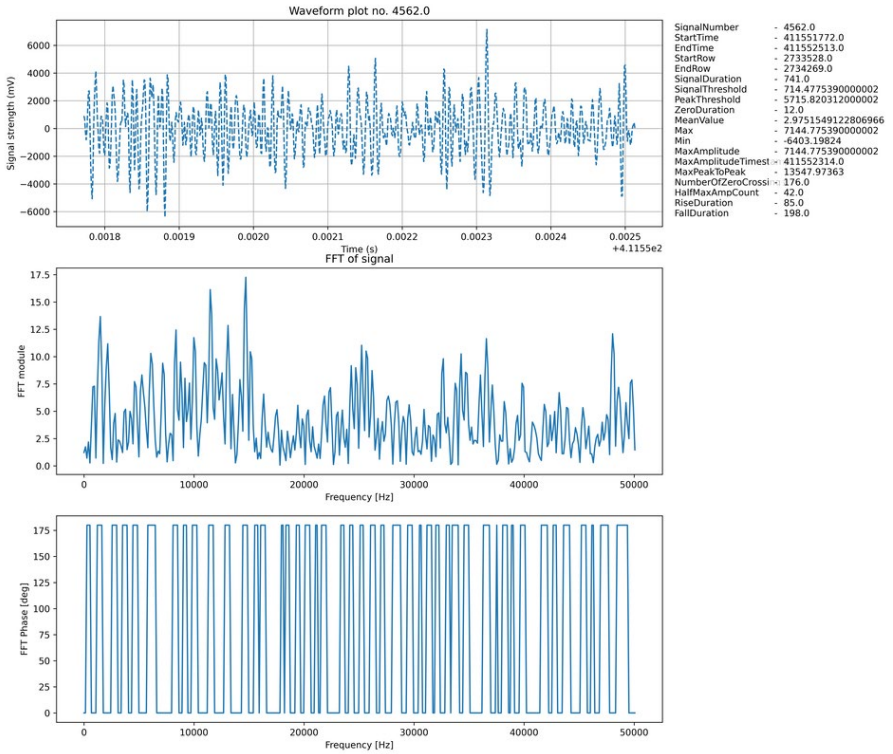

Figure 10. FFT signal from test A1.

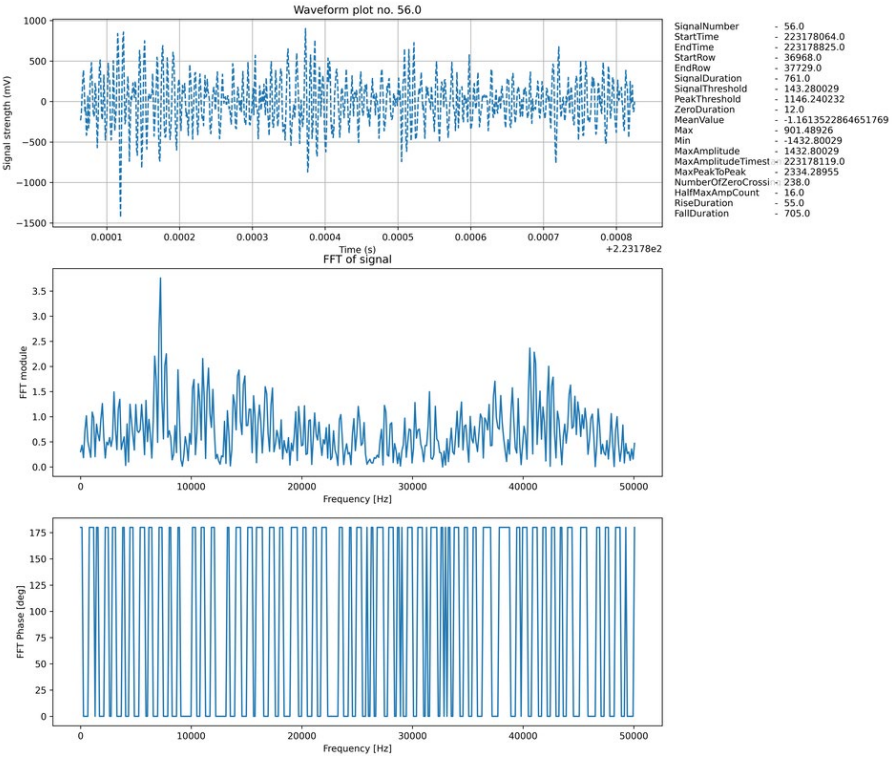

Figure 11. FFT signal from test B1.

3.5. Waveform statistics across several tests

Statistics across several tests are collected and given in Tables 2 and 3. The data in the tables show a relationship between signal type and the number of hits per waveform. The results indicate that signal A was the most abundant type while type C is the least. The only exception was that no signal type B and C were identified in test B1 from sensor 1 (left-hand sensor in Figure 3(a)). The specimen in test A1 has the highest hits in all signal types, which can be due to the layer of coatings that crack and generates more activity during specimen deformation. Since in the experiments, a force was applied to the point with equal distance between the two sensors, the sensors should record similar waveform data.

Table 2. Number of hits per waveform type from sensor 1 for zero duration of 12 μs.

Test ID	Number of hits per waveform type					
	A	B	C	E	Unknown	Sum
A1	4364	37	9	202	411	5023
A3	561	7	0	65	114	747
B1	111	0	0	5	6	122
B2N	284	3	1	19	40	347

Table 3. Number of hits per waveform type from sensor 2 for zero duration of 12 μs.

Test ID	Number of hits per waveform type					
	A	B	C	E	Unknown	Sum
A1	4306	58	5	209	430	5008
A3	505	5	1	40	56	607
B1	172	1	0	16	33	222
B2N	235	2	3	7	17	266

4. Conclusions

Observing the promising trends of AE technology, the study reported in this article attempted to develop methods and algorithms to analyze the AE signal characteristics for use in monitoring offshore structures. The process started with merging signal data extracted from AEwin, and computer programs were developed to help identify relevant waveforms. Upon processing and highlighting the original data, the different signal signatures were categorized. An algorithm with a defined set of rules was applied to this data and signals to enable grouping the signals and visually representing in waveform and scatter figures. The program managed to create visualizations of waveforms to look for signal properties that could identify signal types. The main conclusions drawn from the study are:

1. The complexity of signal processing was greater than anticipated. Developing tools for classifying signals required a lot of effort leaving limited time to analyze and understand the signals. For instance, a waveform representing yielding was not identified even on tests that were expected to contain it. The program is ready to do the analysis, but depending on how the yield waveform is captured, the classification algorithm may need to be adjusted to appropriately identify this type.
2. The work reported in this article managed to identify many different categories of signals and it is believed that with better test-data, the program should be able to identify signal characteristics with even more precision. After implementation and testing in multiple iterations, the results showed good improvement and more signals were correctly classified. As many signals were not classified, a need for a configurable margin of error became apparent. However, there is still a need to develop efficient algorithms to leverage collected data and characterize data signatures that are sensitive to operational, environmental, and sustainable processes.
3. AET is to some extent capable to detect yielding, as can be seen in Figures 5(a) and (b), where the signal intensity increases at the yield point.

4. Coated specimens (at least brittle preservation coating) produce a high number of crack-like waveforms compared to non-coated specimens. This can be seen by comparing tests A1 and A3, in Tables 2 and 3. Other coating types may behave differently.
5. When comparing signals arriving at two sensors an equal distance from the point of force application, the number of signals of each type are comparable, but not precisely the same. Differences can, for instance, be explained by sensors being different and not picking up signals in the same way.
6. The data used in this project had a cut-off such that signals were limited to 1024 data points where 256 of them were ahead of the signal threshold point. This was too short to see the full shape of many of the recorded signals.
7. In hindsight, a zero duration of 12 μs is too short and will result in chopping a signal pulse into several signals – which is not physical.

It is shown that the development of field monitoring for offshore structures can lead to enhancements in sensor technology and monitoring systems and further provide a reliable standardization for a set of instructions and design of the AE technology. However, there is a need to develop efficient algorithms to leverage collected data and characterize data signatures that are sensitive to operational, environmental, and sustainable processes.

Acknowledgement: The technical support provided by Jørgen Grønsund, Khaled Dawood, Svein Anfinnsen and the laboratory engineers at DNV are highly appreciated.

References

[1] Grigorian H, Scherf I, Yu W C and Christensen Ø 2001 Cost-efficient structural upgrade and life extension of Ekofisk platforms with use of modern reassessment techniques, *Offshore Technology Conf.*, Houston, Texas, April 2001.
[2] Vestli H 2016 *Structural Health Monitoring of Offshore Jackets.* MSc. Thesis, University of Stavanger, Norway.
[3] Lee A, Wang G, Ternowchek S and Botten S F 2004 Structural health monitoring on ships using acoustic emission testing, *The Ship Structure Committee Symposium: Vessel Safety & Longevity through Ship Structure Research.* (Linthicum, USA: 18–20 May 2014).
[4] Duthie D B and Gabriels F 2014 Remote monitoring of offshore structures using acoustic emission, *Proc. of 11th European Conf. on Non-Destructive Testing,* 2014.
[5] Vestli H, Lemu H G, Svendsen B T, Gabrielsen O and Siriwardane S C 2017 Case studies on structural health monitoring of offshore bottom-fixed steel structures. In *The 27th Int. Ocean and Polar Engineering Conf. (ISOPE)*, 2017.
[6] INSPECTIONEERING.COM. 2020. *Overview of Condition Based Monitoring (CBM)* [Online]. Available: https://inspectioneering.com/tag/condition+based+monitoring [Accessed, 08.21].
[7] Khaled D 2019 *Acoustic Emission Testing for Offshore Jacket strutures.* MSc. Thesis, University of Stavanger, Norway.
[8] En D 2005. Hot Rolled Products of Structural Steels Part 2: Technical Delivery Conditions for Non-Alloy Structural Steels. *DIN EN*, 10025-2.
[9] Standard N 2000 Material data sheets for structural steel. *Norway Technology Center, N-0306 Oslo, Norway*.
[10] Nguyen B G N 2020 *Study of the characteristics of acoustic emission signals*, MSc thesis, University of Stavanger, Norway.